Pure Appl. Geophys. 168 (2011), 2277–2288

DOI 10.1007/s00024-011-0266-6

Pure and Applied Geophysics

Breaking Up: Comminution Mechanisms in Sheared Simulated Fault Gouge

K. Mair[1,2] and S. Abe[3]

Abstract—The microstructural state and evolution of fault gouge has important implications for the mechanical behaviour, and hence the seismic slip potential of faults. We use 3D discrete element (DEM) simulations to investigate the fragmentation processes operating in fault gouge during shear. Our granular fault gouge models consist of aggregate grains, each composed of several thousand spherical particles stuck together with breakable elastic bonds. The aggregate grains are confined between two blocks of solid material and sheared under a given normal stress. During shear, the grains can fragment in a somewhat realistic way leading to an evolution of grain size, grain shape and overall texture. The 'breaking up' of the fault gouge is driven by two distinct comminution mechanisms: grain abrasion and grain splitting. The relative importance of the two mechanisms depends on applied normal stress, boundary wall roughness and accumulated shear strain. If normal stress is sufficiently high, grain splitting contributes significantly to comminution, particularly in the initial stages of the simulations. In contrast, grain abrasion is the dominant mechanism operating in simulations carried out at lower normal stress and is also the main fragmentation mechanism during the later stages of all simulations. Rough boundaries promote relatively more grain splitting whereas smooth boundaries favor grain abrasion. Grain splitting (plus accompanying abrasion) appears to be an efficient mechanism for reducing the mean grain size of the gouge debris and leads rapidly to a power law size distribution with an exponent that increases with strain. Grain abrasion (acting alone) is an effective way to generate excess fine grains and leads to a bimodal distribution of grain sizes. We suggest that these two distinct mechanisms would operate at different stages of a fault's history. The resulting distributions in grain size and grain shape may significantly affect frictional strength and stability. Our results therefore have implications for the earthquake potential of seismically active faults with accumulations of gouge. They may also be relevant to the susceptibility of rockslides since non-cohesive basal shear zones will evolve in a similar way and potentially control the dynamics of the slide.

Key words: Comminution, Fracture, Fault gouge, Friction, Abrasion, Fragmentation.

[1] Physics of Geological Processes, University of Oslo, P.O. Box 1048, Blindern, 0316 Oslo, Norway. E-mail: karen.mair@fys.uio.no

[2] *Present Address*: Department of Geosciences, University of Oslo, P.O. Box 1047, Blindern, 0316 Oslo, Norway.

[3] Geologie-Endogene Dynamik, RWTH Aachen University, Lochnerstrasse 4-20, 52056 Aachen, Germany. E-mail: s.abe@ged.rwth-aachen.de

1. Introduction

Faults are often filled with granular debris or fault gouge material that accumulates between the walls of a fault as it slides. The evolution state of this gouge, including the grain size and shape distribution, and the structures formed therein, affects the frictional properties, and hence sliding behaviour of the fault. Fragmentation processes operating in this granular gouge material during shear, change the shapes (e.g. Storti *et al.*, 2007; Heilbronner and Keulen, 2006; Stünitz *et al.*, 2010) and grain size distributions (e.g. Sammis *et al.*, 1987; Blenkinsop, 1991; Rawling and Goodwin, 2003; Storti *et al.*, 2003; Billi, 2005; Keulen *et al.*, 2007; Sammis and King, 2007) of the gouge grains. One feature that many fault gouges have in common is that the grain size distribution follows a power law. In such cases, the presence of survivor (or relic) grains (Engelder, 1974; Cladouhos, 1999), i.e. large grains that appear to survive deformation almost intact and retain much of their original mass, is common.

Power law size distributions have been observed in natural fault gouges (e.g. Sammis *et al.*, 1987; Blenkinsop, 1991; Storti *et al.*, 2003), in synthetic fault gouge generated in laboratory experiments (Marone and Scholz, 1989; Biegel *et al.*, 1989) and have also been reproduced in numerical models (Abe and Mair, 2005; Mair and Abe, 2008). Theoretical models of grain fragmentation in sheared granular gouge (Sammis *et al.*, 1987; Sammis and King, 2007) indicate that progressive intra(trans)-granular fracture, that is most likely for nearest neighbour grains of similar sizes, can drive the evolution of the grain size distribution to a power law with an exponent of $D = 2.6$ at small strains and $D = 3.0$ at high strains. To explain field observations of $D > 3.0$ and highly rounded grains occurring in glacial tills and natural

fault gouges, it has been suggested (Hooke and Iverson, 1995; Storti *et al*., 2003; Rawling and Goodwin, 2003) that under certain conditions, grain boundary abrasion may be an important additional comminution process. It can, therefore, be stated that the comminution mechanisms operating during the deformation of a fault gouge leave a signature in the grain shape and size distribution which can be observed. The combined analysis of size distribution and shape (e.g. Hooke and Iverson, 1995; Heilbronner and Keulen, 2006; Storti *et al*., 2007; Bjørk *et al*., 2009) can, therefore, be an effective method that can help constrain potential fragmentation mechanisms.

The key importance of understanding comminution mechanisms and their influence on the evolution of fabrics in a sheared fault gouge lies in their potential control on the mechanical properties of the gouge. Experimental work using synthetic fault gouge has shown that the grain size distribution influences strength (Henderson *et al*., 2010) and sliding stability (Mair *et al*., 2002). Two-D DEM simulations (e.g. Morgan, 1999) also suggest that grain size distribution may influence friction. In addition, it has been shown that grain shape has a first order influence of the sliding friction of the fault gouge. This has been demonstrated experimentally (Mair *et al*., 2002; Frye and Marone, 2002; Anthony and Marone, 2005) and also in 3D numerical models of fault gouge (Abe and Mair, 2009).

In previous work we have developed a 3D numerical model of granular fault gouge with breakable gouge grains (Abe and Mair, 2005). This model has been used to investigate the evolution of grain size and deformation localization in fault gouge (Mair and Abe, 2008) and the influence of grain shape on gouge friction (Abe and Mair, 2009). In both areas, the numerical modeling results have been shown to match experimental data very well, thereby validating the model as an important tool for the investigation of fault gouge processes. In this paper, we use the model to look in detail at the comminution mechanisms operating while the gouge is sheared. One of the key advantages of the numerical simulation approach for the investigation of processes occurring inside fault gouge is that we can directly track gouge grain motions, fracture and interactions at any instance and their evolution with accumulated slip. These data are often difficult to obtain directly from laboratory experiments conducted at realistic stress conditions, or from field observations of natural faults.

As a result of our numerical simulations, we demonstrate two distinct comminution mechanisms, grain splitting and grain abrasion, that are favored at different normal stress and boundary roughness conditions and lead to the development of distinct grain size distributions. We also show that the relative importance of the two mechanisms can change with accumulated strain as the fault gouge evolves.

2. Method

To model the fragmentation of fault gouge, which is an inherently discrete problem, we use a discrete element (DEM) approach (Cundall and Strack, 1979; Mora and Place, 1994; Place and Mora, 1999). The DEM approach has successfully been used to investigate various aspects of fault gouge processes in 2D (e.g. Aharonov and Sparks, 1999; Morgan, 1999) and more recently 3D (e.g. Hazzard and Mair, 2003), but these studies have generally involved minimal evolution of the individual gouge grains. In our new 3D simulations, fault gouge grains are modeled as aggregates (Abe and Mair, 2005) composed of many (up to 10,000) individual particles bonded together with breakable elastic bonds (Fig. 1). A bond model including normal, shear, bending and torsion forces (Wang *et al*., 2006) has been used. If particles which are not bonded together come into contact, for example, after the bond between them has been broken, they interact by linear elastic and frictional forces (Place and Mora, 1999; Abe and Mair, 2005). When a bond failure threshold is exceeded, the aggregate grains can fracture, permitting gouge evolution in a somewhat natural way. For the remainder of the paper we will refer to "particles" as the fundamental unit of the discrete model and "grains" as aggregates of connected particles (this includes original grains and the daughter fragments produced by fragmentation). Particles have a radii between 0.2 and 1 model unit and initial

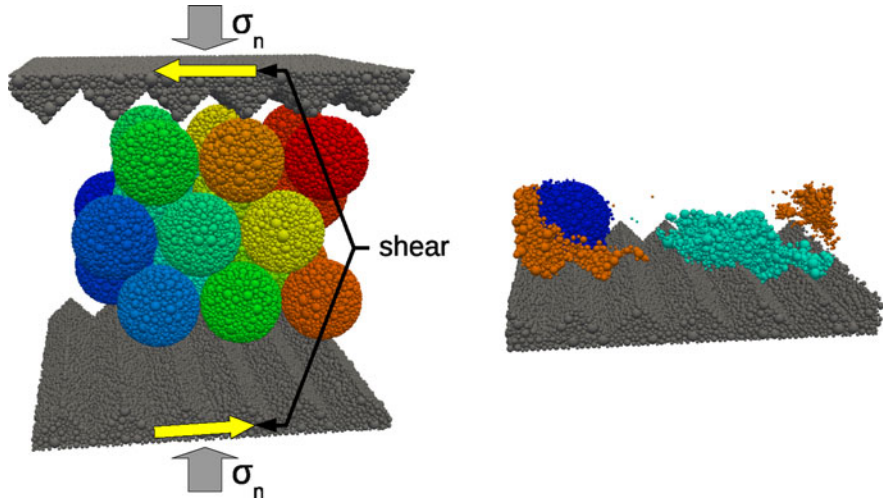

Figure 1
Initial setup (*left*) of a typical fault model. Aggregate gouge grains are composed of individual particles bonded together that can break apart with shearing. *Arrows* indicate the sense of shear, σ_n indicates applied normal stress. Final state (*right*) of the model after engineering shear strain of approximately 4 at a normal stress of 30 MPa. The *upper* boundary block and most grains are removed to reveal comminuted grains

aggregate grains have an approximate radius of 8 model units.

To enable the simulation of sufficiently large models, the parallel DEM simulation package ESyS-Particle (Abe *et al.*, 2003) (http://launchpad.net/esys-particle/) has been used. The main computations were performed on a compute cluster at the Norwegian Center for High Performance Computing (NOTUR) consisting of Intel Xeon based compute nodes (Xeon X5355, 2.66 GHz) and an Infiniband interconnect. Typical model runs, e.g. Model III in Table 1, took around 1,800 CPU hours on this system, either 140–150 h on 12 CPU cores (St002-St008, St037) or 105 h on 18 CPU cores (St044).

We use initially spherical aggregate grains constrained between rigid upper and lower boundary blocks (or fault walls) as shown in Fig. 1. Spherical grains were chosen to mimic laboratory experiments on spherical glass beads (Mair *et al.*, 2002; Frye and Marone, 2002; Anthony and Marone, 2005) and hence allow proper model validation. The model has repeating boundaries right and left, frictionless walls front and back, and either rough or smooth upper and lower walls. Under constant normal stress (σ_n), shear is applied to the upper and lower boundaries (see arrows in Fig. 1). Shearing rate is increased linearly to the chosen velocity (over the initial 0.05 shear strain) then held constant for the duration of the simulation. Top and bottom walls move in the normal direction in order to maintain the pre-defined normal stress. For all simulations we constantly monitor stresses and displacements at the boundaries of our model as well as tracing individual particle positions, motions and interactions. Macroscopic friction is calculated from the shear divided by the normal forces acting on the upper and lower boundary blocks (for details see (e.g. Mair and Abe, 2008; Abe and Mair, 2009).

We have conducted an extensive series of simulations to investigate the influence of applied normal stress, accumulated strain and boundary (wall) roughness on grain fragmentation processes. In addition, we have conducted ensembles of simulations (i.e. repeats with different random seeds for the sphere packing process used to generate the aggregate grains) at specific conditions to test the reproducibility of our results. Details are summarized in Table 1.

To track the fracture of aggregate grains and distinguish between different comminution mechanisms, we analyzed the relative size of daughter grains produced in each grain breaking event. Individual grains are identified by post-processing snapshots of the simulation data (saved at pre-determined time intervals) to determine which particles are still connected by bonds. For details of the

Table 1

Numerical simulations

Simulation	Initial aggregate grains	Normal stress (MPa)	Walls	Shear displacement	Strain (%)	Surface generated ($t = 10^6$)	Splitting fraction % ($t = 10^6$)
I (B013)	27	10	Smooth	188	219	34,044	1.48
I (B014)	27	15	Smooth	159	222	46,893	8.58
I (B015)	27	20	Smooth	147	225	57,271	16.8
I (B016)	27	30	Smooth	176	281	61,620	27.2
II (S011)	30	10	Rough	82.5	263	5,164	30.6
II (S012)	30	15	Rough	82.5	334	9,728	39.5
II (S013)	30	20	Rough	82.5	351	11,847	40.1
II (S014)	30	25	Rough	82.5	367	13,810	44.1
II (S015)	30	30	Rough	82.5	381	15,782	33.0
III (St044)	51	5	Rough	93.5	205	4,515	1.9
III (St002)	51	15	Rough	93.5	264	12,069	26.7
III (St003)	51	15	Rough	93.5	247	10,480	24.3
III (St004)	51	15	Rough	93.5	240	9,285	20.6
III (St005)	51	15	Rough	93.5	257	11,509	27.9
III (St006)	51	15	Rough	93.5	254	11,578	23.2
III (St007)	51	15	Rough	93.5	264	12,507	32.3
III (St008)	51	15	Rough	93.5	270	13,863	29.4
III (St037)	51	30	Rough	93.5	318	24,471	24.8
IV (St038)	81	25	Rough	93.5	230	57,484	29.5

The models fall into four groups: (I) Models B013-B016 having smooth boundaries, an identical model geometry consisting of 241,506 particles, and varying normal stress; (II) Models S011-S015 with rough boundaries, identical model geometry with 122,170 particles, and differing normal stress; (III) Models St002-St008, St037 and St044 with rough boundaries, where St002, St037 and St044 use the exact same geometry with 185,958 particles and different normal stresses, whereas St003-St008 (deformed at a given normal stress) use similar model geometries with 185,400–186,300 particles based on different random realizations of the same general setup to test reproducibility; and (IV) Model St038 is a larger (i.e. higher resolution) realization of a rough boundary setup using 4,81,832 particles. The column 'splitting fraction (%)' describes the percentage of the total surface generated by comminution that is due to grain splitting

procedure, see Abe and Mair (2005); Mair and Abe (2008). After identifying which particles belong to an individual grain, the grain mass can be calculated by summing up the relevant particle masses. From this we can calculate grain size distributions which we generally present as equivalent grain diameter (i.e. the diameter of a sphere of equivalent mass). As noted in Abe and Mair (2005), we do not plot grains with equivalent diameter less than 1 model unit since the size distribution of this fraction is dominated by single particles and hence an artifact of the initial particle set up and not the grain fracturing process. Comminution events are found by comparing the grains identified in consecutive snapshots. We classify grain splitting events as those where the largest of the daughter fragments is smaller than 80 percent (mass) of the original grain, see Fig. 2, left. The other events are classified as grain abrasion. The new grain surface area generated by a comminution event is calculated by determining which bonds have been broken between particles in different daughter grains during the event and adding up the surface area generated. The surface area A generated by each of the broken bonds is calculated from the average radius r_{avg} of the particles involved as $A = \pi r_{avg}^2$. In the literature it is often assumed that the energy needed to create a new fracture is proportional to its surface area (Wilson *et al.*, 2005; Chester *et al.*, 2005 and references therein). We, therefore, use the relative amounts of new surface area created by the different comminution mechanisms as a proxy for the work partitioning between them and thus a measure of their relative importance.

Herein we will refer to breaking up of aggregate grains (when the fracture mechanism is not specified) as fragmentation, comminution or grain breakage. Specific grain breakage mechanisms will be referred to as grain splitting or grain abrasion according to the definition above.

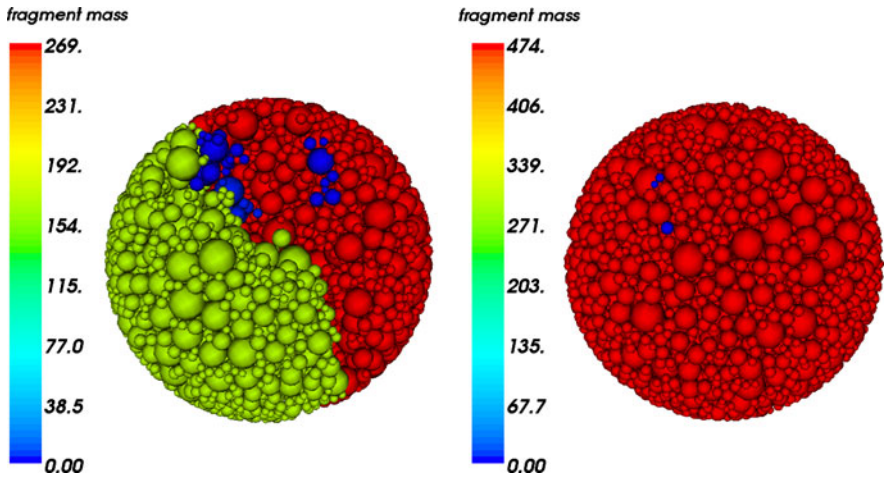

Figure 2
Grain splitting (*left*) and grain abrasion (*right*) events are illustrated. Grain fragments are colored according to their mass

3. Results

3.1. Grain breakage

The grain breakage occurring in our simulations with accumulated shear strain is now presented as new grain surface generated versus simulation time. Data from simulations with smooth (Fig. 3) and rough (Fig. 4) upper and lower walls, and low (10 MPa) and high (30 MPa) normal stresses are presented. For valid comparison between simulations with slightly different initial model geometries (e.g. different sphere packing used to generate the initial aggregate grains) all data are scaled by the total number of particles that make up the gouge grains in a given simulation. At low (10 MPa) normal stresses, shown in Figs. 3a and 4a, simulations produce a background level of grain breakage that persists throughout shear and is punctuated by episodic spikes indicating enhanced breakage. There is no consistent evolution of grain breakage rate with accumulated strain. At the same shearing rate but higher (30 MPa) normal stress (Figs. 3b, 4b), significantly more surface area is generated suggesting that more grain breakage occurs. Although comminution continues throughout the simulation, it is initially high, then decays monotonically with accumulated slip. These first order observations appear to hold for simulations having smooth (Fig. 3) and rough (Fig. 4) upper and lower walls.

The grain breakage occurring during different simulations is now summarized as total (scaled) surface area generated in a given simulation in Fig. 5. For all simulation conditions, the total surface area generated increases systematically as a function of increasing applied normal stress. This indicates that higher normal stresses promotes a higher intensity of comminution and more grain breakage as might be expected. The total surface area generated for a given normal stress varies a little between the different models, with smooth boundary models (I) and rough boundary models (II) plotting relatively high compared to models (III) and (IV). This suggests some sensitivity to boundary roughness as well as the details of the individual model geometries.

3.2. Grain Splitting Versus Grain Abrasion

The relative importance of the different comminution mechanisms, classified as grain splitting or grain abrasion in the manner described above, is highlighted in Figs. 3, 4, 6 and 7. The nature of comminution is quite distinct at low and high normal stress and shows some dependence on wall roughness. At low (10 MPa) normal stresses (Figs. 3a, 4a), comminution is mainly expressed as a background of grain abrasion events generating a relatively constant mean level with a few episodic grain splitting events but that otherwise appear to contribute little to the fragmentation. In contrast, at high (30 MPa) normal

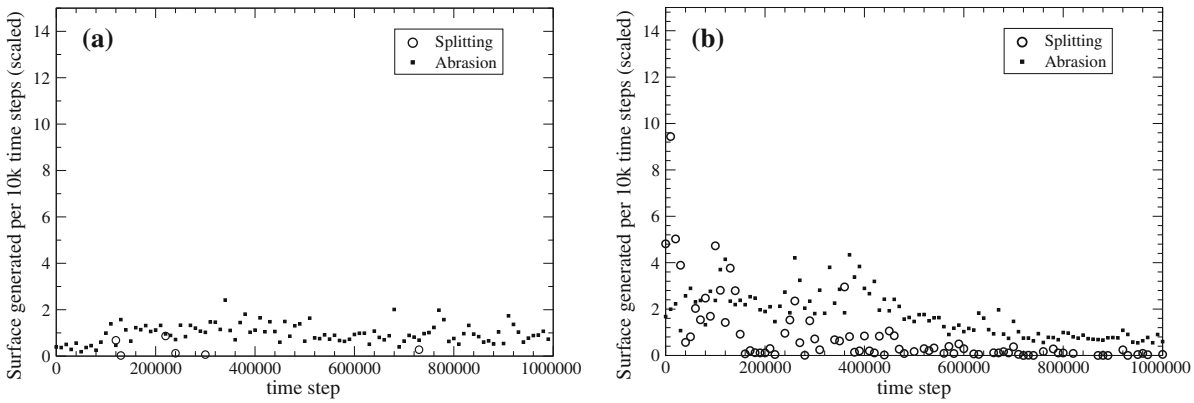

Figure 3

Grain breakage is presented as new surface generated (per 10,000 time steps) versus simulation time step for simulations having smooth fault walls (model I) and applied normal stresses of: **a** 10 MPa, and **b** 30 MPa. After the initial load up, which comprises the initial 10,000 timesteps, the simulation time is equivalent to accumulated slip. Grain splitting (*circles*) and grain abrasion (*squares*) events are distinguished as defined in the main text (The surface generated is scaled by number of particles in the gouge layer)

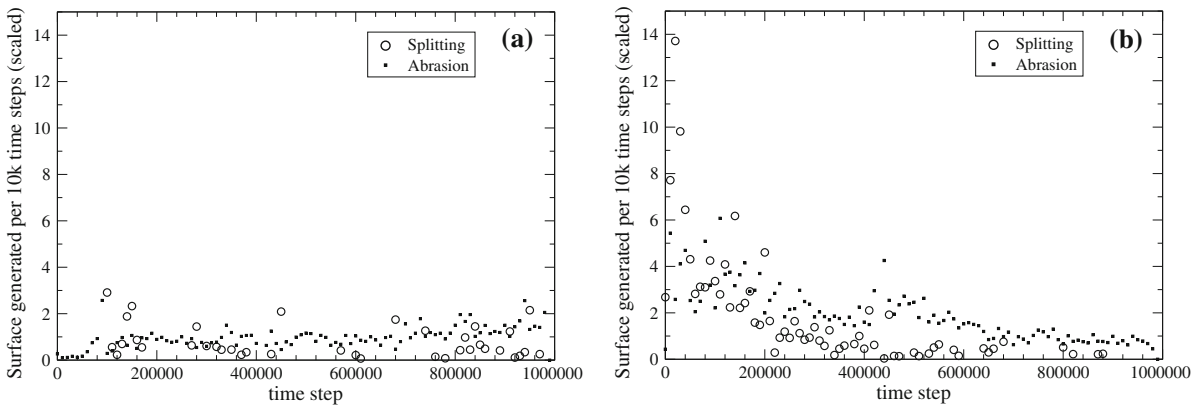

Figure 4

Grain breakage plotted as new surface generated (per 10,000 time steps) versus simulation time. Simulations have rough fault walls (model II) and applied normal stresses of: **a** 10 MPa, and **b** 30 MPa. After the initial load up, which comprises the initial 10,000 timesteps, the simulation time is equivalent to accumulated slip. Grain splitting (*circles*) and grain abrasion events (*squares*) are distinguished (The surface generated is scaled by number of particles in the gouge layer)

stress (Figs. 3b, 4b), grain splitting events are more prevalent, particularly in the initial stages of the simulation. As strain accumulates, with the exception of a few episodic events, grain splitting decays more rapidly than grain abrasion and abrasion returns as the dominant comminution mechanism.

The fraction (percentage) of new surface that is generated by grain splitting during the simulations is summarized in Fig. 6 for a range of normal stress and boundary roughness conditions. In general, the fraction of events identified as grain splitting increases with applied normal stress. In addition, the fraction of splitting events appears to be sensitive to boundary roughness, with rough boundaries promoting relatively more grain splitting for a given normal stress. A reduction in the fraction of grain splitting events observed at highest stress is seen in models (II) and (III). This may be linked to a 'splitting saturation' effect where splitting is suppressed when grain size evolves to a particular size distribution.

The relative importance of grain splitting versus abrasion for different normal stresses as a function of simulation time (i.e. accumulated strain) is summarized in Fig. 7a, b for smooth and rough walls respectively. Changes in model thickness that essentially correspond to compaction and hence porosity

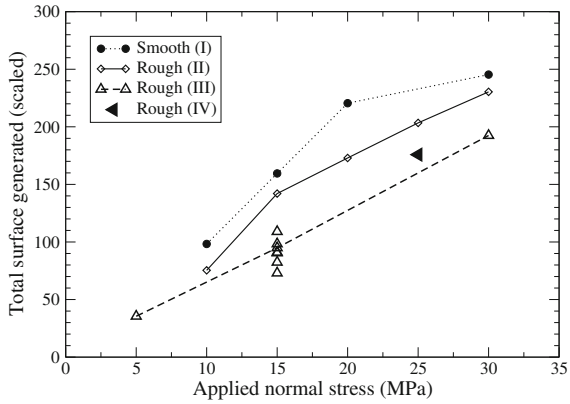

Figure 5
Total surface area generated during simulation as a function of normal stress. Data are shown for simulations having smooth (model I) and rough (model II, III, IV) *upper* and *lower* walls. See Table 1 for model details. (The surface generated is scaled by number of particles in the gouge layer)

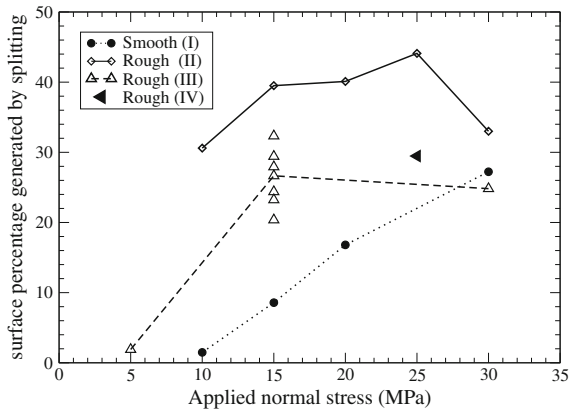

Figure 6
Summary of the fraction of new surface (in percent) generated by grain splitting events occurring during simulations as a function of applied normal stress. Data are presented for simulations having smooth (model I) and rough (model II, III, IV) *upper* and *lower* walls. See Table 1 for model details

changes during the simulations are also plotted. Data show that in general, grain splitting plays a larger role at high normal stresses and for rough boundaries, as was shown in the bulk measurements (Fig. 6). More importantly, we see that the relative fractions of splitting and abrasion evolve with time (i.e. accumulated strain) in a way that is quite distinct from each other and is sensitive to both normal stress and boundary roughness. In the simulations at higher normal stress where grain splitting plays a significant role, the peak in grain splitting occurs early and is generally lagged by the peak in grain abrasion suggesting a gradual shift in the dominant comminution mechanism with accumulated strain.

The amount of new surface generated by grain abrasion and the evolution of the abrasion signal with time (i.e. accumulated strain) is quite similar for simulations having rough and smooth walls. Grain splitting, however, is generally more prevalent in the rough boundary simulations. Interestingly, the peak values of grain splitting achieved in the rough and smooth simulations are not dramatically different but for rough boundary cases, elevated levels of grain splitting are maintained for a longer time (i.e. more strain) resulting in a greater overall contribution from the grain splitting mechanism.

Simulations compact with shear to a degree that depends on normal stress (Fig. 7). Compaction rate is largest initially, coincident with major fracturing events, decaying with strain in a similar manner as the fracturing also decays. Spikes in the fracturing intensity (in both splitting and abrasion) are often associated with inflections in the model thickness curve however this association has not been investigated quantitatively.

3.3. Grain Size Distributions

The evolution of grain size distribution with accumulated shearing is a result of comminution. It is intrinsically linked to both the intensity of comminution, and the relative importance of the two comminution mechanisms we have identified above. In Fig. 8 we show the evolution of grain size distribution as a function of increasing amounts of strain. Plots show non-cumulative number of grains versus equivalent grain diameter for: (a) low (10 MPa); and (b) high (30 MPa) normal stress at increasing simulation time increments (t) corresponding to increasing amounts of strain. The initial grain size distribution in the simulations ($t = 0$, solid square symbol) consists of mono-disperse grains of diameter 9 model units.

The low stress simulation (Fig. 8a) shows the rapid development of a grain size that approaches a bimodal distribution. With increasing strain, the largest grains reduce in size a little whilst a new set of fine fragments develops. There is a notable

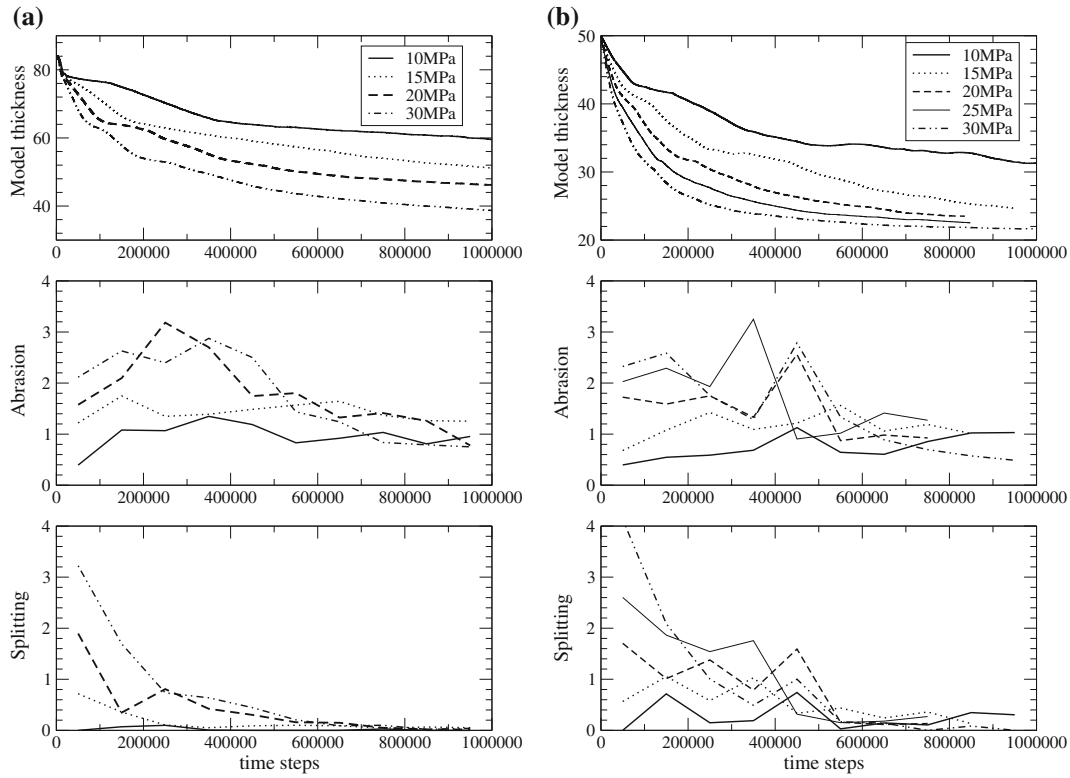

Figure 7
Model thickness (*top plot*), the surface generated by grain abrasion (*middle plot*) and grain splitting (*lower plot*) events as a function of time (strain) during simulations carried out at normal stresses of 10–30 MPa for: **a** smooth (model I) and **b** rough (model II) walls. The surface generated (labelled on *y*-axes as 'abrasion' or 'splitting') is scaled by number of particles in the gouge layer and averaged over 100,000 time steps

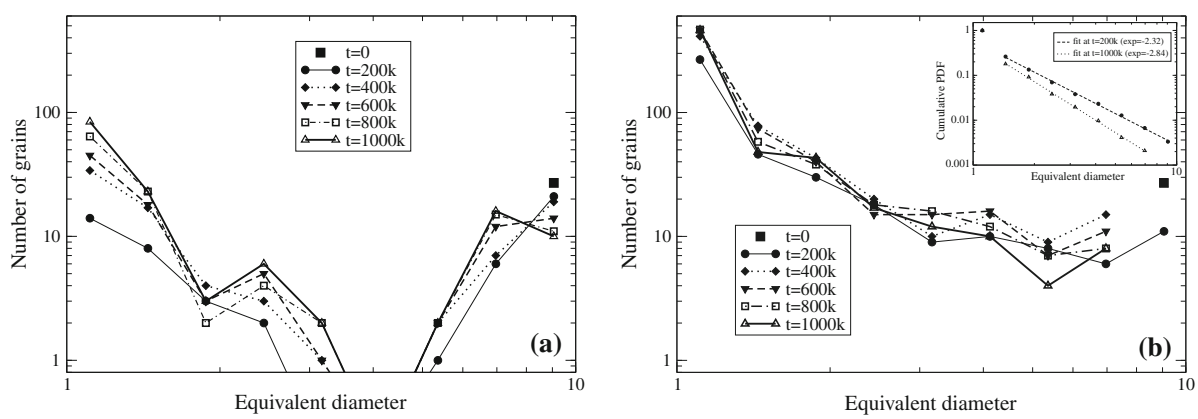

Figure 8
Grain size distributions produced with increasing simulation time steps (t = Xk = X,000 time steps), plotted as non-cumulative frequency by number versus equivalent grain diameter for: **a** 10 MPa, and **b** 30 MPa applied normal stress. The data shown are for simulations having smooth walls (model I). The initial grain size distribution ($t = 0$) is shown in both plots as *squares*. The *inset* to **b** shows the data for t = 200k (200,000 timesteps) and t = 1,000k (1,000,000 timesteps) plotted as cumulative probability density. These datasets can be approximated by a power law with exponent 2.32 and 2.84, respectively

absence of intermediate sized grains even at the largest strains reached in our simulations. In contrast, at high normal stress (Fig. 8b) grain size rapidly evolves (even at $t = 200k$) into a wide size distribution that can be approximated (see inset) by a power law with exponent 2.32. As simulation time (strain) increases, the larger size fractions are depleted slightly and more fine fragments are produced, leading to a distribution (at $t = 1{,}000k$) that is approximated by a power law with exponent 2.84. In both cases (Fig. 8a, b, a number of survivor grains are present even at the late stages of the simulations.

4. Discussion

Our models of gouge fragmentation during shear show that comminution is sensitive to applied normal stress, accumulated strain, and the roughness of upper and lower boundary walls. Comminution intensity, i.e. the amount of new surface generated per unit of shear strain, is systematically greater under higher normal stresses as might be expected. We demonstrate two distinct comminution mechanisms, grain splitting and grain abrasion, that are favored for different normal stress, boundary roughness and accumulated slip conditions. In the context of previous work, grain splitting could be considered equivalent to intra-granular or trans-granular fracture, whereas grain abrasion would encompass grain boundary abrasion, flaking at grain edges and spalling. At low normal stresses, grain abrasion is the dominant comminution mechanism and persists at a more or less constant level throughout our simulations. High normal stresses, promote significant grain splitting, particularly in the initial stages of simulations, that decays with accumulated strain.

In simulations where grain splitting is significant, we observe a transition from splitting dominated comminution to abrasion dominated comminution with accumulated strain, indicating that comminution processes may change as a fault zone evolves. A switch or competition between a splitting (trans-granular) type breakage mechanism and abrasion type mechanism has previously been suggested from micro-structural observations of sheared glacial tills (Hooke and Iverson, 1995) laboratory and natural faults (e.g. Storti *et al*., 2003; Rawling and Goodwin, 2003; Hayman, 2006; Keulen *et al*., 2007; Bjørk *et al*., 2009) and basal shear zones of rockslides (Henderson *et al*., 2010). Our observations certainly support these interpretations, and indicate scenarios where a given comminution mechanism is likely to be favored.

The implementation of rough grooved walls in our simulations offers a situation which matches laboratory experiments (Mair *et al*., 2002; Frye and Marone, 2002; Anthony and Marone, 2005), and though inherently complicated, may be close to the situation in many natural faults. We have previously shown (Abe and Mair, 2009) that to get realistic values of friction matching laboratory experiments, rough walls, and angular gouge fragments are required. It should be noted that the effect of the boundary shape might be larger in these models than it is in real fault gouge, since the roughness is relatively large with respect to the width of the fault zone. Also, our fault boundaries (like those in laboratory experiments (e.g. Mair *et al*., 2002; Frye and Marone, 2002; Anthony and Marone, 2005) are indestructible whereas in a real fault zone, rough walls would themselves fracture, become entrained into the gouge layer and potentially become more smooth with accumulated strain. Smooth boundary walls, though a simplified case, are a scenario that also matches particular laboratory conditions (Anthony and Marone, 2005) and may have relevance for mature natural fault zones.

Total comminution for a given normal stress is similar for both rough and smooth walls (Fig. 5) with smooth walls producing slightly more comminution. This highlights the influence that small differences in contact configurations between gouge grains and fault walls may play. The contribution to comminution from grain splitting is larger for simulations with rough boundary walls (Figs. 6, 7), whereas smooth walls promote relatively more grain abrasion. Intuitively this makes sense given the rough boundary grooves that can potentially penetrate into and split the grains quite effectively. Alternatively, grains and fragments could become trapped in the grooves and hence potentially more susceptible to shear enhanced splitting. Since grain splitting persists for longer (i.e. larger strains) in rough walled simulations (Fig. 7),

we suggest that the strain at which the transition from splitting to abrasion occurs may be influenced by the roughness of the fault walls.

Grain size distribution evolves with comminution in a way that is sensitive to normal stress, accumulated strain and hence the comminution mechanisms operating. A bimodal size distribution is developed in simulations carried out at low normal stress where grain abrasion dominates. We therefore interpret a bimodal grain size distribution to be the fragment size evolution "signature" of grain abrasion in the absence of major grain splitting events. The rapid development of a wide (power law) grain size distribution in the initial stages of high normal stress simulations where grain splitting dominates, suggests that such a size distribution is intrinsically linked to progressive grain splitting. This fits with expectations of the size distribution produced by a constrained comminution model (Sammis *et al*., 1987). However, as our results show, grain abrasion has contributed to the total comminution and resulting grain size distribution. The low normal stress simulations we have presented show less efficient grain size reduction than higher stress scenarios; however, we note that a significant fraction of fine fragments are produced by this mechanism.

In addition to being a product of comminution, evolving grain size distributions may themselves influence subsequent comminution. Our observations of exponential decay in grain splitting with increasing strain, indicate that the intra-granular fracture condition is being reached in fewer and fewer grains. We suggest a "splitting saturation" is reached when grain size evolves to a particular size distribution. This is likely due to changes in the local contact force network that one might expect with evolving grain size distributions (e.g. Mair and Hazzard, 2007). Highly focussed force chains (grain bridges) carry enhanced stress through sheared granular materials where neighboring grains have similar sizes (i.e. initial stages of simulations) leading to a high grain splitting potential. In contrast, granular materials with wide size distribution where large grains are surrounded by smaller ones (such as those found in the later stages of our simulations) host much more diffuse force networks that effectively buffer the large grains from high stresses, hence reducing their fracture potential. In this scenario, grain sliding and abrasion would instead be favored.

The models presented here have some limitations. Despite the fact that we are using parallel computation, the size of the models is limited to a few hundred thousand particles. This results in a grain size range which is only slightly larger than one order of magnitude, i.e. the ratio between the initial grain diameters and our "grinding limit" is smaller than may be expected in a natural fault gouge (e.g. An and Sammis, 1994). This may have an influence on the breaking mechanisms of the small to intermediate sized particles which is difficult to quantify. Further, we present comminution as generated new surface binned per 10K timesteps. This gives an indication of relative importance of the different comminution mechanisms; however, we acknowledge that such a method could be biased by the exact binning chosen. The surface area based method of measuring comminution may also potentially give extra weight to "flaking" events where slivers of material with high aspect ratios are dislodged.

Despite these limitations, our simulations offer some indication of how fragmentation processes may operate in faults. Our results support ideas that constrained comminution involving progressive trans(intra)-granular fracturing may be a necessary condition for faults to achieve power law size distributions. However, once the power law distribution is established, grain abrasion would potentially become the dominant mechanism and by producing excess fine fragments, provide a valid way to obtain the high D-values often observed in the field (e.g. Hooke and Iverson, 1995; Storti *et al*., 2003; Hayman, 2006). At low stresses, granular flow involving grain abrasion is a potential way to change grain size distributions in situations where intragranular fracture is not possible (Rawling and Goodwin, 2003). Interestingly, if a natural fault gets smoother with increasing strain and the grain size of the gouge evolves to a wide size distribution, this would potentially provide two drivers to promote a grain abrasion as the dominant comminution mechanism operating with accumulated strain. Extensive grain abrasion will most likely round both survivor grains and small fragments that surround them, potentially providing a way to significantly affect

mechanical strength of shear zones at either low stress or high strains (e.g. HENDERSON *et al*., 2010).

5. Conclusions

We show that comminution occurs in sheared simulated fault gouge with accumulated strain. Grain breakage is driven by two distinct comminution mechanisms: grain splitting and grain abrasion. The relative importance of these mechanisms depends on applied normal stress, boundary wall roughness and accumulated strain. Grain splitting contributes significantly to comminution at high stresses, especially in the initial stages of simulations, whereas grain abrasion dominates at lower stress and during the later stages of all conditions. Rough fault walls promote grain splitting whereas smooth fault walls favor grain abrasion. Grain splitting is an efficient driver for rapidly developing a wide (power law) grain size distribution, whereas grain abrasion tends to produce a bimodal grain size distribution that has a distinct lack of intermediate sized grains. The apparent switch in comminution mechanism from splitting to abrasion with accumulated strain (at high stresses) may be driven by a changing local stress network associated with evolving grain size distributions. Although grain splitting is significantly more efficient at grain size reduction and producing a classic power law size distribution, we show that grain abrasion operating at lower stresses (or at later stages of simulations) produces accumulations of fine grains and will most likely round the large survivor fragments. This could potentially affect the mechanical properties of faults even at relatively low stress where significant grain breakage is not anticipated. The processes we describe have clear implications for the frictional stability of faults containing granular gouge material and also the susceptibility of rockslides due to the evolution of debris filled basal shear zones.

Acknowledgments

Computations were made using NOTUR (Norwegian National High Performance Computing) resources (project nn4557k). We thank everyone who has contributed to the development of the ESyS-Particle software, in particular, Shane Latham, Dion Weatherley, Paul Cochrane and David Place. We thank the referees and editor whose comments helped improve the paper. This work was supported by a Center of Excellence grant from the Norwegian Research Council to PGP (Center for Physics of Geological Processes) at the University of Oslo.

References

ABE, S. and K. MAIR: 2005, '*Grain fracture in 3D numerical simulations of granular shear*'. Geophys. Res. Lett. *32*.

ABE, S. and K. MAIR: 2009, '*Effects of gouge fragment shape on fault friction: New 3D modelling results*'. Geophys. Res. Lett. *36*.

ABE, S., D. PLACE, and P. MORA: 2003, '*A Parallel Implementation of the Lattice Solid Model for the Simulation of Rock Mechanics and Earthquake Dynamics*'. Pure. Appl. Geophys. *161*.

AHARONOV, E. and D. SPARKS: 1999, '*Rigidity phase transition in granular packings*'. Physical Review E *60*(6), 6890–6896.

AN, L. and C. G. SAMMIS: 1994, '*Particle-size Distribution of cataclastic Fault Material from southern California - a 3-D Study*'. Pageoph *143*(1–3), 203–227.

ANTHONY, J. and C. MARONE: 2005, '*Influence of particle characteristics on granular friction*'. J. Geophys. Res. *110*.

BIEGEL, R. L., C. G. SAMMIS, and J. H. DIETERICH: 1989, '*The frictional properties of a simulated gouge having a fractal particle distribution*'. J. Struct. Geol. *11*, 827–846.

BILLI, A.: 2005, '*Grain size distribution and thickness of breccia and gouge zobes from thin (<1 m) strike-slip fault cores in limestone*'. Journal of Structural Geology *27*, 1823–1837.

BJØRK, T. E., K. MAIR, and H. AUSTRHEIM: 2009, '*Quantifying granular material and deformation: Advantages of combining grain size shape and mineral phase recognition analysis*'. Journal of Structural Geology *31*.

BLENKINSOP, T. G.: 1991, '*Cataclasis and Processes of Particle Size Reduction*'. Pageoph *136*(1), 59–86.

CHESTER, J., C. F.M., and A. KRONENBERG: 2005, '*Fracture surface energy of the Punchbowl fault, San Andreas system*'. Nature *437*, 133–135.

CLADOUHOS, T. T.: 1999, '*Shape prefered orientations of survivor grains in fault gouge*'. Journal of Structural Geology *21*, 419–436.

CUNDALL, P. A. and O. STRACK: 1979, 'A discrete numerical model for granular assemblies'. *Géotechnique* **29**, 47–65.

ENGELDER, J. T.: 1974, '*Cataclasis and Generation of Gault Gouge* '. Geol. Soc. Am. Bull. *85*(10), 1515–1522.

FRYE, K. M. and C. MARONE: 2002, '*The effect of particle dimensionality on granular friction in laboratory shear zones*'. Geophys. Res. Lett. *29*(19).

HAYMAN, N.: 2006, '*Shallow crustal fault rocks from the Black Mountain Detachments, Death Valley, CA*'. Journal of Structural Geology *28*, 1767–1784.

HAZZARD, J. F. and K. MAIR: 2003, '*The importance of the third dimension in granular shear*'. Geophys. Res. Lett. *30*(13).

HEILBRONNER, R. and N. KEULEN: 2006, '*Grain size and grain shape analysis of fault rocks*'. Tectonophysics *427*(1–4), 199–216.

HENDERSON, I. H. C., G. V. GANEROD, and A. BRAATHEN: 2010, '*The relationship between particle characteristics and frictional strength in basal fault breccias: Implications for fault-rock evolution and rockslide susceptibility*'. Tectonophysics *486*, 132–149.

HOOKE, R. L. and N. IVERSON: 1995, '*Grain-size distribution in deforming subglacial tills: Role of grain fracture*.' Geology *23*(57–60).

KEULEN, N., R. HEILBRONNER, H. STÜENITZ, A.-M. BOULLIER, and H. ITO: 2007, '*Grain size distributions of fault rocks: A comparison between experimentally and naturally deformed granitoids*'. Journal of Structural Geology *29*, 1282–1300.

MAIR, K. and S. ABE: 2008, '*3D numerical simulations of fault gouge evolution during shear: Grain size reduction and strain localization*'. *Earth Planet. Sci. Lett. 274*, 72–81.

MAIR, K., K. FRYE, and C. MARONE: 2002, '*Influence of grain characteristics on the friction of granular shear zones*'. J. Geophys. Res. *107*(B10).

MAIR, K. and J. F. HAZZARD: 2007, '*Nature of stress accommodation in sheared granular material: Insights from 3D numerical modeling*'. Earth Planet. Sci. Lett. *259*(3-4), 469–485.

MARONE, C. and C. SCHOLZ: 1989, '*Particle-size distribution and microstructures within simulated fault gouge*'. Journal of Structural Geology *11*(7), 799–814.

MORA, P. and D. PLACE: 1994, '*Simulation of the Frictional Stick-slip Instability*'. Pure Appl. Geophys. *143*, 61–87.

MORGAN, J. K.: 1999, '*Numerical simulations of granular shear zones using the distinct element method, 1. Shear zone kinematics and the micromechanics of localization*'. J. Geophys. Res. *104 B2*, 2,703–2,718.

PLACE, D. and P. MORA: 1999, '*The lattice solid model: incorporation of intrinsic friction*'. J. Int. Comp. Phys. *150*, 332–372.

RAWLING, G. C. and L. B. GOODWIN: 2003, '*Cataclasis and particulate flow in faulted, poorly lithified sediments*'. Journal of Structural Geology *25*, 317–331.

SAMMIS, C., G. KING, and R. BIEGEL: 1987, '*The Kinematics of Gouge Deformation*'. Pageoph *125*(5), 777–812.

SAMMIS, C. G. and G. C. P. KING: 2007, '*Mechanical origin of power law scaling in fault zone rock*'. Geophys. Res. Lett. p. L04312.

STORTI, F., F. BALSAMO, and F. SALVINI: 2007, '*Particle shape evolution in natural carbonate granular wear material*'. TERRA NOVA *19*(5), 344–352.

STORTI, F., A. BILLI, and F. SALVINI: 2003, '*Particle size distributions in natural carbonate fault rocks: insights for non-self-similar cataclasis*'. Earth Planet. Sci. Lett. *206*, 173–186.

STÜNITZ, H., N. KEULEN, T. HIROSE, and R. HEILBRONNER: 2010, '*Grain size distribution and microstructures of experimentally sheared granitoid gouge at cocsiesmic slip rates—Criteria to distinguiesh seismic and aseismic faults*.' Journal of Structural Geology *32*, 59–69.

WANG, Y., S. ABE, S. LATHAM, and P. MORA: 2006, '*Implementation of particle-scale rotation in the 3-D lattice solid model*'. Pageoph *163*, 1769–1785.

WILSON, B., T. DEWERS, Z. RECHES, and J. BRUNE: 2005, '*Particle size and energetics of gouge from earthquake rupture zones*'. Nature *434*(7034), 749–752.

(Received July 1, 2010, revised November 4, 2010, accepted November 16, 2010, Published online February 15, 2011)